Proceeding *20th SEAGC - 3rd AGSSEA Conference in conjunction with 22nd Annual Indonesian National Conference on Geotechnical Engineering.* Jakarta - INDONESIA, 6 -7 November 2018. ISBN No. 978-602-17221-6-9

Dynamic *p-y* Curves for a Single Pile by 1g Shaking Table Tests

S.S. Jeong[1] and H.S. Lim[1]
[1]*Department of Civil and Environmental Engineering, Yonsei University, Seoul, Republic of Korea*
E-mail: soj9081@yonsei.ac.kr

ABSTRACT: In this study, dynamic p-y curves were suggested for pseudo-static analysis from 1g shaking table tests under various loading frequencies. Based on the results of the model tests, the dynamic p-y curves are highly dependent on the relationships between the natural frequency of the soil-pile systems and the loading frequency. The dynamic p-y curves were proposed as hyperbolic functions. The ultimate soil resistance and the initial soil stiffness were developed as functions of the properties of the pile and soil. Based on comparisons with the existing p-y curves, the proposed dynamic p-y curve was demonstrated to be capable of predicting the behaviour of a pile under dynamic loads.
Keywords: Dynamic p-y curve, loading frequency, initial soil stiffness, ultimate soil resistance, Pseudo-static analysis.

1. INTRODUCTION

Seismic design has become increasingly important, because the number of large-scale earthquakes has increased worldwide to reduce the threat that earthquake-induced structural deformation and damage. Pseudo-static analysis, which is a method of converting dynamic loads into the equivalent static loads, is widely used in the seismic design of pile foundations. The p-y curves considering nonlinear behaviour of soil are most frequently used for pseudo-static analysis in practical engineering applications. However, the p-y curves, which were proposed by Reese et al. (1974) and API (American Petroleum Institute, 1987), derived from field tests applying static and cyclic loads at the pile head. In other words, the p-y curves do not properly consider soil stiffness and soil inertia effects under seismic loads. Therefore, the p-y curves are not suitable for application to seismic design of pile foundations.

Much work has been done on pile foundations subjected to dynamic loads. Ting et al. (1987) noted that the secant slope of the dynamic p-y curve is highly dependent on the loading frequencies in dynamic pile load tests. Dou and Byrne (1996) showed that API p-y curves underestimate the lateral soil stiffness or resistance under strong shaking intensities. The NCHRP (National Cooperative Highway Research Program, 2001) described that the dynamic behavior of the soil-pile interaction is closely associated with the pile diameters, shear wave velocities of the soil and loading frequencies. Additionally, the NCHRP suggested dynamic p-y curves by using a numerical analysis method that related the static p-y curves to the dimensionless frequency. However, the verification of the dynamic p-y curves was conducted under restrictive conditions by statnamic tests in which a lateral load was applied on a pile head. El Naggar and Bentley (2000) observed that the soil resistance under dynamic loading increases due to the damping effect. They also noted that the dynamic p-y curves depended on the loading frequency. Therefore, it is necessary to study dynamic p-y curves for seismic design of pile foundations.

The objective of this study is to develop dynamic p-y curves for pseudo-static analysis by using model tests under various loading frequencies based on the natural frequencies of soil-pile systems.

2. 1G SHACKING TABLE TESTS

2.1 Test set-up and programs

The dynamic model tests were conducted by 1g shaking table tests. The size of the soil box was 1,200×600×800 mm with sponge pads 50 mm thick on the sidewalls to reduce reflection waves during shaking (Fig. 1). The model pile was made of aluminium alloy with a hollow circular section. The size of the model pile was applied the similitude law proposed by Iai (1989). The properties of the model pile are summarized in Table 1. Jumoonjin sand, characterized as clean and uniform sand, was used in the tests. The properties of jumoonjin sand are listed in Table 2.

Fig. 1 shows the sectional view of 1g shaking table tests. The displacement of the pile was measured by two LVDTs (linear variable differential transformers) located on either side of the pile cap. In other to obtain the bending moments, strain gauges were installed along the pile. Accelerometers were installed on the superstructure and within the soil of to measure the natural frequencies of the soil-pile system and the free field displacement.

Sweep tests were conducted to evaluate the natural frequencies of the soil-pile systems under various conditions. The input wave was as a sine wave and applied approximately 5 seconds. The loading frequencies used in the tests were calculated from the natural frequencies (fn) of the soil-pile systems. The natural frequencies range from 0.4fn Hz to 1.6fn Hz. The amplitude accelerations ranged from 0.098g to 0.4g.

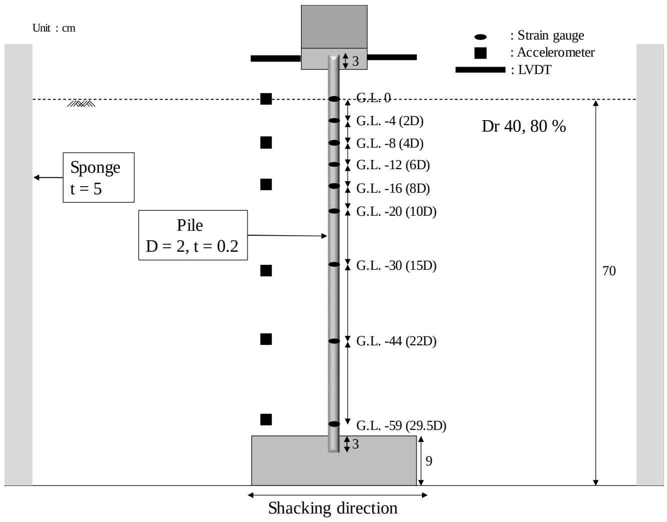

Figure 1 Sectional view of 1g shaking table test

Table 1 Pile Properties

Pile	Scaling factor (Iai, 1989)	Prototype	Model pile
Diameter (cm)	λ	91.44	2.0
Thickness (cm)	λ	1.4	0.2
Pile depth (m)	λ	1,710	64
Flexural rigidity (kN·m^2)	$\lambda^{4.5}$	842,983	0.31995

*Note: Scaling factor λ = 26.72

Table 2 Properties of Test Soil

USCS	D_{10} (mm)	D_{60} (mm)	C_u	G_s	$\gamma_{d,max}$ (t/m^3)	$\gamma_{d,min}$ (t/m^3)
SP	0.38	0.49	1.59	2.65	1.62	1.36

2.2 Determination of experimental dynamic *p-y* curves

The experimental dynamic *p-y* curves were derived from the bending moments along the depth of the pile. The bending moment profile along the pile was double differentiated and integrated to the obtain soil resistance (*p*) and lateral pile deflection (y_{pile}) according to simple beam theory, as shown in Eq. (1) and Eq. (2):

$$p = \frac{d^2M(z)}{dz^2} \tag{1}$$

$$y_{pile} = \int \frac{M(z)}{EI} dz \tag{2}$$

where *p* is the soil resistance, *M(z)* is the bending moment at depth *z*, y_{pile} is the lateral pile deflection, *EI* is the flexural rigidity of the pile and *z* is the distance along the pile.

The bending moment of the pile foundation were calculated by Eq. (3) using the stain measured by the strain gauges.

$$M = \frac{E\varepsilon I}{y} \tag{3}$$

where *M* is the bending moment, *y* is the distance from the neutral axis, *E* is the Elastic modulus of the pile and *ε* is the strain of the pile.

2.3 Test results

The natural frequencies of the soil-pile systems were determined from sweep tests. Fig. 2 shows the typical fourier transform for a natural frequency of a soil-pile system using sweep tests results. As shown in Fig. 2, the natural frequency of this soil-pile system is 10.86 Hz under an acceleration amplitude of 0.154 g in dense sand.

Fig. 3 shows change in the natural frequency with the acceleration amplitude of the soil-pile systems. As the acceleration amplitude increases the natural frequency of the soil-pile systems decreases due to the reduced elastic modulus of the soil. In addition, the natural frequency of the soil-pile system for the relative density of 40 %, is smaller than that for the relative density of 80 % due to the increased stiffness in the soil with a higher relative density.

Fig. 4 shows dynamic p-y curves under various conditions. As shown in Fig. 4(a), the dynamic p-y curves are flat near the surface and become stiffer with depth because the soil confining stress increases. Fig. 4(b) shows that the lateral pile deflection increases with the acceleration amplitude due to greater inertial forces. The soil resistance also increases with the acceleration amplitude. However, the increments of the soil resistance decreased with the acceleration amplitude. The secant slope of the dynamic p-y curve decreases with an increase in the acceleration amplitude. As shown in Fig. 4(c), The dynamic p-y curve is closely related to the ratio of the loading frequency to the natural frequency. As the frequency ratio approaches 1.0, the lateral deflection further increases, and the slope of the dynamic p-y curve decreases due to resonance.

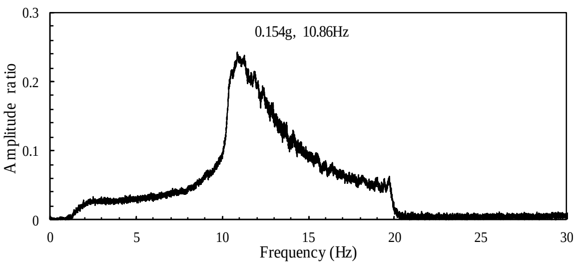

Figure 2 Typical Fourier transform for natural frequency of soil-pile system

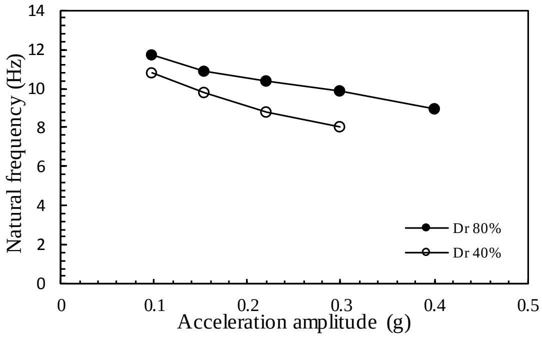

Figure 3 Natural frequency of soil-pile systems at various acceleration amplitudes

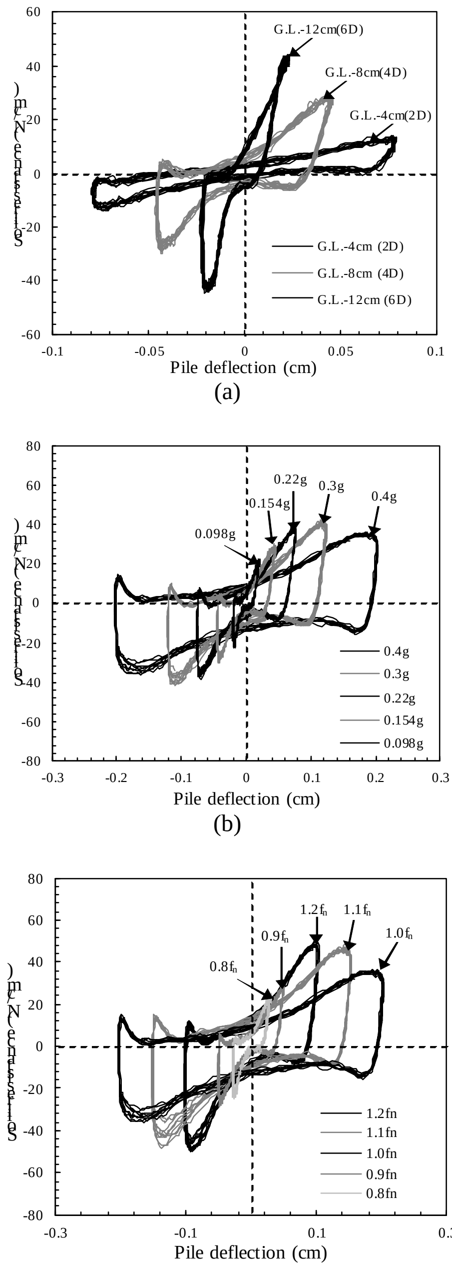

Figure 4 Experimental dynamic *p-y* curves: (a) with different depth (b) with various acceleration amplitudes (c) with various loading frequencies

3. PROPOSED DYNMAIC *P-Y* CURVES

Based on the experimental dynamic p-y curves, the simplified dynamic p-y backbone curve was suggested for pseudo-static analysis under various loading frequencies. All of the peak points of the experimental dynamic p-y curves corresponding to the maximum soil resistance, were collected at several depths and plotted on a p-y plane. The dynamic p-y backbone curves were fitted to this data.

In this study, the general shape of experimental dynamic p-y curves for dry sand were fit mathematically by a hyperbolic function. The best fit curve was the hyperbolic function of Kondner (1963):

$$p = \frac{y}{\dfrac{1}{K} + \dfrac{y}{p_u}} \quad (4)$$

where p is the soil resistance, y is the lateral pile deflection, K is the initial soil stiffness and p_u is the ultimate soil resistance. Generally, the shape of the hyperbolic curve is controlled by the value of p_u and K. Therefore, these values were proposed from model tests.

Figs. 5 show the peak points of the experimental dynamic p-*y* curves and the dynamic *p-y* backbone curves, which were determined by regression analysis. As shown in Fig. 5, the results indicate nonlinearity of the soil-pile system, and the hyperbolic function accurately reflects the experimental results. Additionally, the initial slope (K) and the ultimate soil resistance (p_u) increased with depth due to confining stresses of soil. In this study, the initial soil stiffness and the ultimate soil resistance were suggested to be a function of the confining pressure and the Rankine's passive pressure coefficient, respectively.

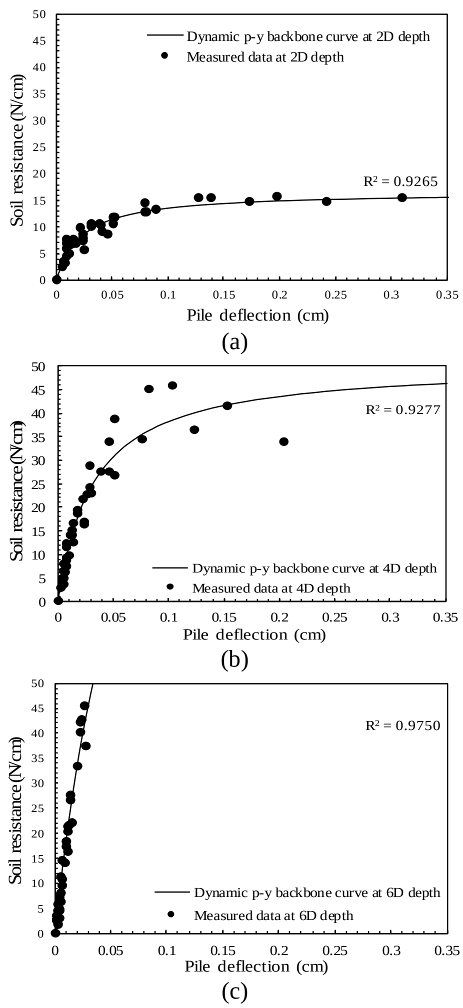

Figure 5 Dynamic *p-y* backbone curve at dense sand: (a) at 2 pile diameter; (b) at 4 pile diameter; (c) at 6 pile diameter

3.1 Ultimate soil resistance

Kim et al. proposed the ultimate soil resistance based on Rankine's passive earth pressure. The best-fit ultimate soil resistance was determined by using Eq. (4).

$$\frac{p_u}{D} = AK_p\gamma' z^n \quad (4)$$

where D is pile diameter, K_p is Rankine's passive pressure coefficient, is effective unit weight, z is depth of soil and A, n are curve fitting parameters. In order to determine the curve fitting parameters A and n, Eq. (4) was normalized in logarithm as Eq. (5):

$$\log\left(\frac{p_u}{D}\right) = n\log(z) + \log(AK_p\gamma') \quad (5)$$

Fig. 6 shows the soil resistance in transformed coordinates from the model test results. From the linear regression analysis, empirical equations for the soil resistance were obtained as Eqs. (6) and (7):
The soil resistance for dense sand:

$$\frac{p_u}{D} = 7.10K_p\gamma' z^{1.97} \quad (6)$$

The soil resistance for loose sand:

$$\frac{p_u}{D} = 8.21K_p\gamma' z^{1.88} \quad (7)$$

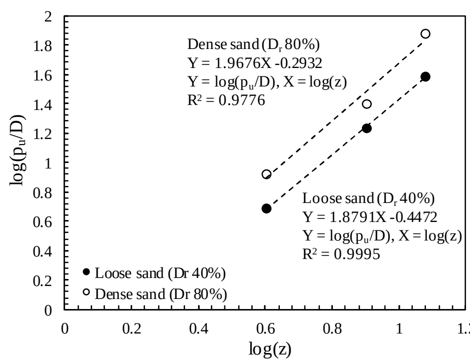

Figure 6 Determination of ultimate soil resistance

3.2 Initial soil stiffness

The variation of the initial tangent modulus with confining pressure is represented by an empirical equation proposed by Janbu(1963):

$$K = AP_a\left(\frac{\sigma'}{P_a}\right)^{0.5} \quad (8)$$

where P_a is atmospheric pressure (10.13 N/cm^2), is confining stress and A is a curve-fitting parameter.

A linear regression analysis was used to obtain the best-fit values for the parameter *A*.

Fig. 7 shows the initial soil stiffness in the transformed coordinates from the model test results. Through a linear regression analysis, the curve-fitting parameters of A were determined to be 1,414.8 and 995.94 for the relative densities of D_r 80 % and D_r 40 %, respectively. Based on these results, the empirical equation for K can be rewritten as Eqs. (9) and (10).
The initial soil stiffness for dense sand:

$$K = 1414.8P_a\left(\frac{\sigma'}{P_a}\right)^{0.5} \quad (9)$$

The initial soil stiffness for loose sand:

$$K = 995.94P_a\left(\frac{\sigma'}{P_a}\right)^{0.5} \quad (10)$$

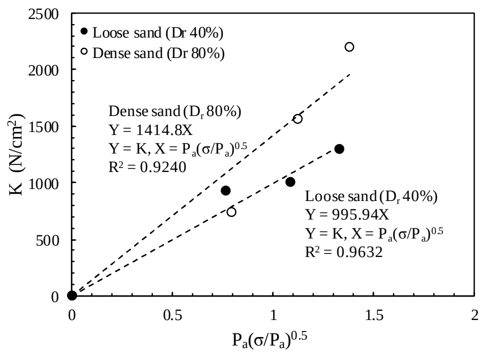

Figure 7 Determination of initial slope

3.3 Application of proposed dynamic *p-y* curves

To verify the applicability of the proposed *p-y* curve more reliably, other test results were compared with proposed dynamic *p-y* curves. Yang (2008) has conducted 1g shaking table tests in dry loose and dense sand. The test soil was Jumoonjin sand and the model pile with hollow circular section was embedded in a soil box (1,800×600 ×1,200 mm) and the embedded depth of pile was 110 cm with a diameter of 3.2 cm. An input sine wave of acceleration amplitude 0.154 g and frequency 6 Hz applied at the bottom of the soil box.

The proposed dynamic p-y curves were validated by pseudo-static analysis with the FB-MultiPier program (2007). The analysis was performed by applying the inertial force determined by the measured acceleration at the surcharge mass and the surcharge mass. Fig 7. shows the predicted and measured bending moment distributions in test piles. The resulting proposed p-y curves predict a trend of the measured bending moment distributions better than the existing p-y curves.

Table 4 Pile Properties and Test Conditions (Yang, 2008)

Pile	Model pile	Test	Condition
Diameter (cm)	3.2	Soil condition	Dr 80%, 40%
Thickness (cm)	0.5		
Pile depth (cm)	110	Frequency (Hz)	6
Flexural rigidity (kN·cm^2)	2764,424	Acceleration (g)	0.154

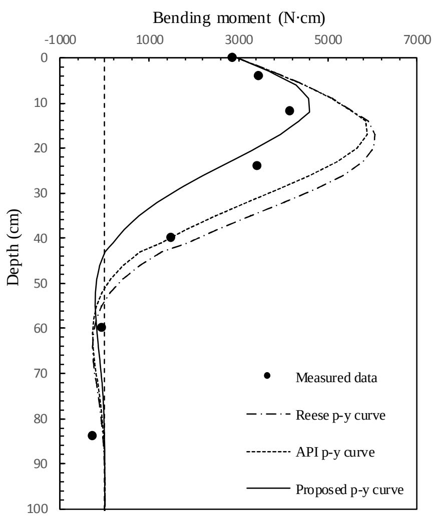

(a)

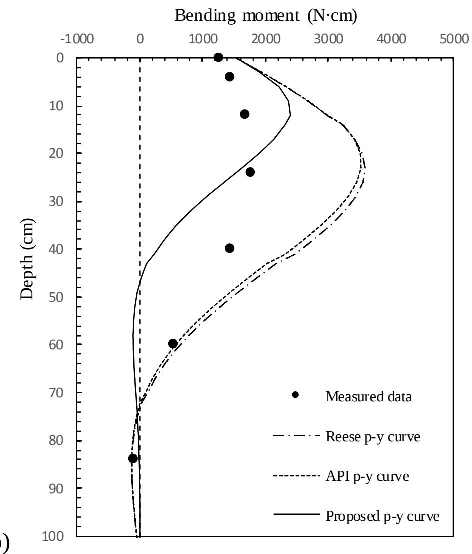

(b)

Figure 7 Comparison of bending moment distributions results of Yang(2008) for application of proposed *p-y* curves

4. CONCLUSION

In this study, a new hyperbolic *p-y* curve was proposed under dynamic loads for piles embedded in dry sand that can apply to pseudo-static analysis. The experimental results confirmed that dynamic *p-y* curves are largely affected by the relationships between the natural frequency of the soil-pile systems and the loading frequencies, the acceleration amplitude. Based on comparisons with the existing *p-y* curves, the proposed dynamic *p-y* curve is shown to be capable of predicting the behavior of the pile under dynamic loads. Therefore, the proposed *p-y* curves are appropriate to represent the behavior of the pile subjected to dynamic loads.

5. REFERENCES

American Petroleum Institute (API). (1987) Recommended practice for planning, designing and constructing fixed offshore platforms, API Recommended Practice 2A (RP 2A), 17th edition, pp 68-71

Bea, R.G., Littom, R., Nour-Omid, S., and Chang, J.Y. (1984) "A specialized design and research tool for the modelling of near-field soil interactions", 16th Offshore Technology Conference, Houston, pp249-252.

Boulanger, R. W., Curras, C. J., Kutter, B. L., Wilson, D. W., and Abghari, A. (1999) "Seismic soil-pile-structure interaction experiments and analyses", Journal of Geotechnical and Geoenvironmental Engineering, 125, Issues 9, pp750-759.

Broms, B. B. (1964) " Lateral resistance of piles in cohesive soils ", J. soil mech. Fdns. Div. ASCE, 90, pp750-759.

Dou, H. and Byrne, P.M. (1996) "Dynamic response of single piles and soil-pile interaction", Canadian Geotechnical Journal, 33, Issues 1, pp80-96.

El Naggar, M. H. and Bentley, K. J. (2000) "Dynamic analysis for laterally loaded piles and dynamic *p-y* curves", Canadian Geotechnical Journal, 37, Issues 6, pp1166-1183.

Hoit M, Hays C, McVay M, Williams M. (2007) The FB-MultiPier v4 program, Bridge Software Institute.

Iai, S. (1989) "Similitude for shaking table tests on soil-structure-fluid model in 1g gravitational field ", Soils and Foundations, 29, Issues 1, pp105-118.

Janbu, N. (1963) " Soil compressibility as determined by oedometer and triaxial test", Proceedings of the European Conference on Soil Mechanics and Foundations Engineering, Wiesbaden, pp19-25.

Kim, Y. H., Jeong, S. S. and Lee, S. J. (2011) "Wedge failure analysis of soil resistance on laterally loaded piles in clay", Journal of Geotechnical and Geoenvironmental Engineering, ASCE, 137, Issues 7, pp53-77

Kim, Y. H., Jeong, S. S. and Won, J. O. (2009) "Effect of lateral rigidity of offshore piles using proposed *p-y* curves in marine clay ", Journal of Marine Geosourses and Geotechnology, 27, Issues 1, pp53-77

Kondner, R.L. (1963) " Hyperbolic stress-strain response: cohesive soils", Journal of Soil Mechanics and Foundation Division, 87, Issues 1, pp115-144.

National Cooperative Highway Research Program (NCHRP) (2001) Static and dynamic lateral loading of pile groups, NCHRP Report 461, Transportation Research Board – National Research Council 2001, pp13-21.

Novak, M. (1974) "Dynamic stiffness and damping of piles", Canadian Geotechnical Journal, 11, pp574-598.

Reese, L. C., Cox, W. R. and Koop, F. D. (1974) " Analysis of laterally loaded piles in sand", Proc. of the 6th Offshore Technology Conference. Houston, Texas, pp473-484.

Rovithis, E., Kirtas, E., and Pitilakis, K. (2009) "Experimental *p-y* loops for estimating seismic soil-pile interaction", Bulletin of Earthquake Engineering, 3, Issues 7, pp719-736.

Thavaraj, T., Finn, W. D. L., and Wu, G. (2010) "Seismic response analysis of pile foundation", Geotechnical and Geological Engineering, 28, pp275-786.

Yang, E. K. (2008) " Evaluation of dynamic *p-y* curves for a pile in sand from 1g shaking table tests", Seoul, Seoul National University [Ph. D dissertation].

Yang, E. K., Kwon, S. Y., Choi, J. I. and Kim, M. M. (2010) " Prediction of the natural frequency of pile foundation system in sand during earthquake", Journal of the Korean Geotechnical Society, 26, Issues 1, pp45-54 (in Korean).

Yoo, M. T., Choi, J. I., Han, J. T. and Kim, M. M. (2013) " Dynamic *p-y* curves for dry sand from centrifuge tests", Journal of Earthquake Engineering, 17, pp1082-1102.